DISTRIBUTION OF DENSITY AND POTENTIAL OF NUCLEAR INTERACTION

V.YU. DENISOV, V.A. NESTEROV

Institute for Nuclear Researches, Nat. Acad. Sci. of Ukraine
(47, Nauky Prosp., Kyiv 03028, Ukraine; e-mail: denisov@kinr.kiev.ua)

UDC 530.145

Interaction potentials between nuclei evaluated with the help of the Skyrme force in the frameworks of the extended Thomas—Fermi (ETF) approximation and the Hartree—Fock—BCS (HF+BCS) theory have been studied in detail. The amplitude of the nuclear part of the interaction potential between nuclei has been shown to grow as the neutron number in colliding isotopes and the parameter of density distribution diffuseness in interacting nuclei increase. The growth of the diffuseness parameter leads to the reduction of the height of the barrier between nuclei, the deepening of the capture well, and the increase of the fusion cross-section. The diffuseness of the nuclear part of the potential evaluated making use of the Skyrme forces has been demonstrated to exceed that of the nucleon density in interacting nuclei by approximately a factor of 1.5 at large internuclear distances. Reasonable values of the diffuseness parameter of the interaction between medium and heavy nuclei lie in the range $a \approx 0.75 \div 0.90$ fm.

1. Introduction

In order to calculate the various characteristics of nuclear reactions, it is necessary to know the potential energy of interaction between nuclei [1–3]. Therefore, both the magnitude and the radial dependence of the interaction potential between nuclei at small internuclear distances are vitally important for the description of the reaction cross-section in the framework of any model.

The nuclear interaction energy is caused by both the Coulomb interaction between protons and the nuclear interaction between nucleons of colliding nuclei [1–3]. The Coulomb interaction between protons in nuclei is described rather well, which cannot be said about the nuclear interaction between nuclei. A rather large number of various approximations for the nucleus–nucleus interaction has been proposed at present [1–8], but they bring about different barrier heights of the nucleus–nucleus fusion reaction [8,9]. The barrier height depends on the ratio between the Coulomb repulsive and nuclear attractive potentials, which act at small distances between the surfaces of interacting nuclei.

The ratio between the collision energy and the barrier height governs the mechanism of a nuclear reaction. In particular, as the collision energy grows, the number of possible reaction channels increases, and the type of dominating channels changes. The accurate knowledge of the interaction potential between nuclei and of the barrier height is a very challenging problem nowadays.

In order to determine the amplitude of the nuclear interaction between nucleons which belong to different nuclei, it is desirable to use the most exact methods that have been developed for the detailed description of various characteristics of the ground and excited nuclear states [10–17]. Using these methods, one can calculate the energy of interaction between nuclei with high accuracy. In this work, we use both the semiclassical and semimicroscopical approaches in order to determine the potential of interaction between nuclei. In the framework of the semiclassical approach, the distributions of the nucleon density of interacting nuclei and the potential energy of their interaction are calculated in the ETF approximation with Skyrme forces. In the semimicroscopical approximation, the distributions of nucleon density in interacting nuclei are determined in the HF+BCS approximation with Skyrme forces, while the potential energy of interaction between nuclei is calculated in the ETF approximation with Skyrme forces. Note that the ETF approximation and the HF+BCS theory with Skyrme forces describe well the nuclear binding energies, the distributions of nucleon

density in nuclei, the root-mean-square radii, and many other characteristics of the ground and excited nuclear states [10–17].

The reactions of subbarrier fusion [1–3, 18–26] are important from the viewpoint of the definition of the nuclear interaction potential, because these reactions are connected with the interaction amplitude and the potential behavior at small distances between nuclei. Now, there is a lot of various models for the description of subbarrier fusion reactions [1–3, 18–26]. In order to describe the value of the fusion cross-section adequately, the fitting of the nucleus–nucleus interaction parameters is often carried out. For example, the analysis of the data concerning the subbarrier fusion of nuclei, fulfilled in works [22–26], gives a rather high value of the diffuseness ($a \approx 0.8 - 1.5$ fm) of the nuclear part of the internuclear potential parametrized in the form of the Woods—Saxon potential. The authors of many other works [1–3,7,18–21] used lower values for the diffuseness of the nuclear part of the interaction potential between nuclei ($a \approx 0.6 - 0.7$ fm) to describe various nuclear reactions. Therefore, the comprehensive study of the diffuseness magnitude for the nuclear part of the interaction potential between nuclei in the framework of various models is of substantial interest. It is also useful to determine the realistic values for the diffuseness of the nuclear part of the interaction potential between nuclei parametrized in the form of the Woods—Saxon potential.

2. Distribution of the Nucleon Density in Nuclei

The radial distribution of the nucleon density in spherical nuclei has been examined in the framework of various approaches [10–17]. The ETF method with Skyrme forces allowed one to describe the density distribution, the binding energies, and other parameters of nuclei making use of the semiclassical approximation [10–14]. Another method to describe various properties of nuclei is the quantum-mechanical self-consistent HF+BCS method with Skyrme forces which takes the coupling forces into account as well [10, 15–27]. The self-consistent HF method describes the distribution of the nucleon density with high accuracy and is entirely microscopic [10,15,17]. This method allowed the majority of various properties of nuclei in the ground and excited states to be described [10,15–17]. The quantum-mechanical HF method is rather complicated; on the contrary, the ETF method is simple and illustrative. Let us compare the radial distributions of neutron and proton densities calculated in the framework of these methods.

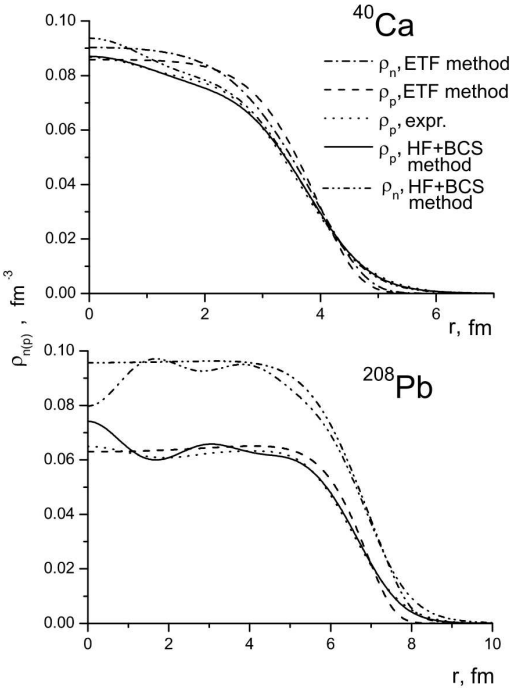

Fig. 1. Radial distributions of the proton and neutron densities in ^{40}Ca and ^{208}Pb nuclei calculated in the framework of the ETF and the HF+BCS methods. The corresponding proton densities are compared with the charge densities derived from the experimental data for electron scattering by those nuclei (*expr*)

The radial distributions of neutron and proton densities in the ground states of ^{208}Pb and ^{40}Ca nuclei, calculated using the ETF approximation with the SkP set of parameters [16] for Skyrme forces, are presented in Fig. 1. The obtained density distributions are compared with the distributions calculated in the self-consistent HF+BCS approximation with the same set of Skyrme force parameters, and with the distributions of charge density derived from the analysis of the experimental data concerning electron scattering by those nuclei [27].

The proton densities calculated in the ETF approximation agree well with both the results of the analysis of experimental data and the densities calculated in the HF approximation. At the same time, the densities found in the framework of the semiclassical approximation fall down more quickly than the experimental or HF+BCS ones in the diffusion range and at large distances. Hence, the value of the diffuseness parameter of the density distribution, which was determined in the ETF approximation, turns out

somewhat smaller than those derived from experimental data or calculated in the quantum-mechanical HF+BCS approximation.

In the region of the diffusive edge of a nucleus, the radial distributions of nucleon density calculated in the HF+BCS approximation agree well with the distributions obtained on the basis of experimental data (see Fig. 1). However, the quantum-mechanical radial distributions of density fluctuate in the internal region of the nucleus with an amplitude that is substantially smaller than the amplitudes of experimentally measured charge densities. The difference between the densities found in the quantum-mechanical and semiclassical approximations is connected not only with the circumstance that the latter does not take shell effects into account, but also because the constant b_1 in the expression for the kinetic energy is equal to $1/36$, in contrast to the quantum-mechanical value of $1/9$ [13], which causes the difference in the asymptotic behaviors of these densities. As a result, the densities calculated in the semiclassical approximation fall down appreciably more quickly at the nucleus edge than those obtained in the framework of the quantum-mechanical HF+BCS approximation (see Fig. 1).

3. Potential Energy of Interaction Between Nuclei

In the framework of the "frozen density" approximation, let us define the potential energy of interaction $V(R)$ between two nuclei positioned at a distance R from each other as the difference of the binding energies $E_{12}(R)$ and $E_1 + E_2$ of the system composed of two nuclei separated by a finite (R) or infinite interval, respectively [8, 9]:

$$V(R) = E_{12}(R) - (E_1 + E_2). \quad (1)$$

The corresponding binding energies of the nuclear system and nuclei 1 and 2 can be found easily making use of the semiclassical expression for the energy density functional if one knows the distribution of nucleon density in the nuclei:

$$E_{12} = \int \varepsilon[\rho_{1p}(\bar{r}) + \rho_{2p}(\bar{r}, R), \rho_{1n}(\bar{r}) + \rho_{2n}(\bar{r}, R)]d\bar{r}, \quad (2)$$

$$E_1 = \int \varepsilon[\rho_{1p}(\bar{r}), \rho_{1n}(\bar{r})]d\bar{r}, \quad (3)$$

$$E_2 = \int \varepsilon[\rho_{2p}(\bar{r}), \rho_{2n}(\bar{r})]d\bar{r} \quad . \quad (4)$$

It is evident that, to determine the potential energy of interaction, we have to know the distribution of nucleon density and the energy density functional. These issues were considered in detail in work [13]. The nucleus–nucleus potential at finite distances between the surfaces of nuclei is caused by the interaction of nucleons in the range of "overlapping tails" of the nucleon density distributions. Therefore, taking the gradient terms in the kinetic energy density into account is very important for the calculation of the potential amplitudes to be accurate.

When nuclei collide, each of them influences the nucleon distribution in the other nucleus through both the Coulomb and nuclear part of the nucleus–nucleus interaction. The "frozen density" approximation adopts that the interaction of nuclei does not affect their nucleon densities. This approximation is obviously justified at the initial stage of the collision, when the nuclear densities overlap weakly, and the interaction of nucleons belonging to different nuclei is small. When heavy nuclei with near-barrier energies collide, the density distributions in them also have no time to change appreciably at the initial stage of the collision. The time of flight t_s across the region of strong interaction between nuclei, $s \approx 3$ fm, can be estimated as $t_s \approx R_t[2\mu s/(e^2 Z_1 Z_2)]^{1/2}$, where R_t is the sum of the nuclear radii, μ is the reduced mass, and Z_1 and Z_2 are the numbers of protons in the interacting nuclei. As a rule, when heavy nuclei collide, $t_s \leq 10^{-21}$ s. The relaxation time for internal nuclear states owing to the nucleon–nucleon interaction can be evaluated as $t_{\rm relax} \approx 2 \times 10^{-22}/e^*$ s [9, 28], where e^* is the energy of excitation per one nucleon in the nuclear system, expressed in MeV. At collisions of two rather heavy nuclei with near-barrier energies, e^* is smaller than $5/A$ MeV, where A is the number of nucleons in the system. Hence, $t_{\rm relax} \approx 0.4 \times A \times 10^{-22}$ s. Therefore, in the case of heavy systems with the number of nucleons of 50 and more, the relaxation time exceeds the time of flight across the region of strong interaction. In this case, the distributions of nucleon density have no time to change substantially during the flight across the region of strong interaction, and the "frozen density" approximation is valid. Since $t_{\rm relax}$ increases with A, the "frozen density" approximation becomes even more justified for heavier systems.

Fig. 2 exhibits the nucleus–nucleus potentials $V(R)$ for ^{16}O—^{16}O, ^{58}Ni—^{58}Ni, ^{118}Sn—^{118}Sn, and ^{208}Pb—^{208}Pb interactions calculated in the framework of the

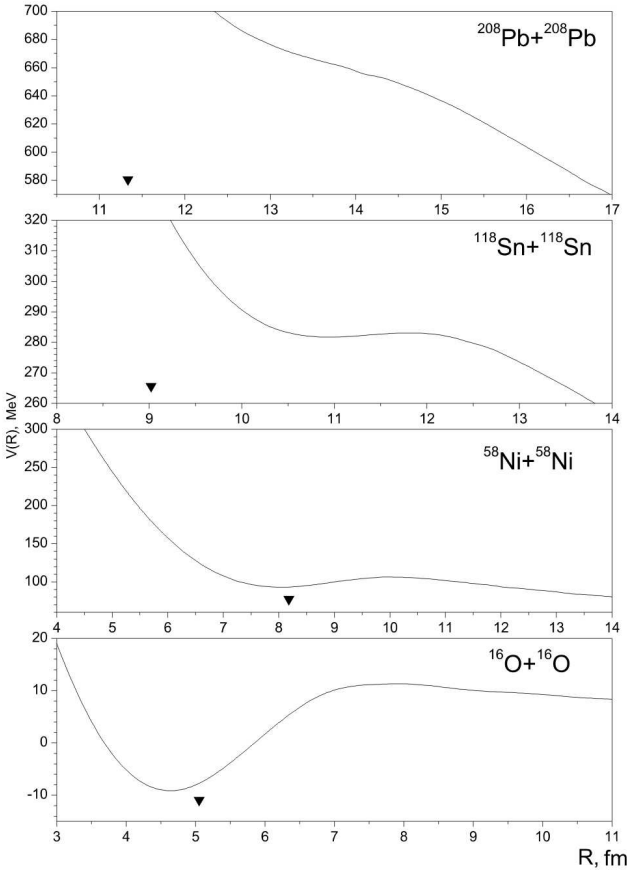

Fig. 2. Potentials of nuclear ^{16}O–^{16}O, ^{58}Ni–^{58}Ni, ^{118}Sn–^{118}Sn, and ^{208}Pb–^{208}Pb interactions calculated in the framework of the ETF approximation. Triangles near the abscissa axes denote the relevant values of the sum of the mean-square radii of colliding nuclei

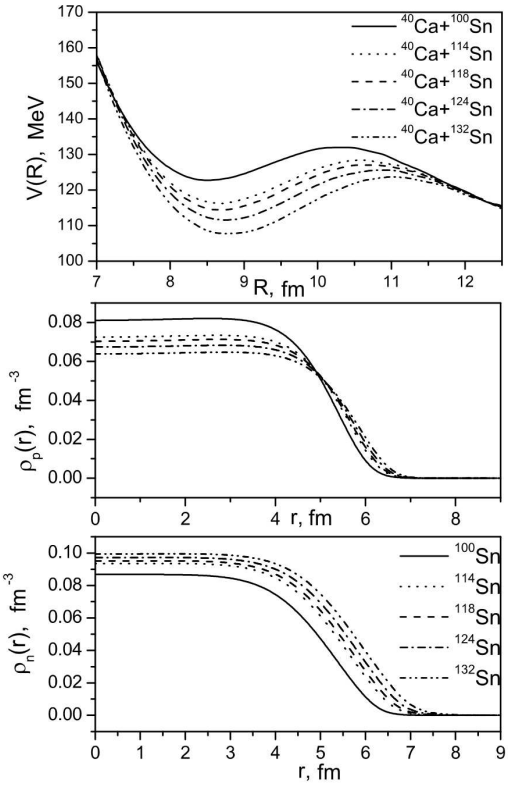

Fig. 3. Interaction potentials $V(R)$ between a ^{40}Ca nucleus and various Sn isotopes and the radial distributions $\rho_p(R)$ and $\rho_n(R)$ of the proton and neutron densities, respectively, in the same isotopes, calculated in the framework of the ETF approximation

ETF approximation. One can see that the depth of the potential capture well appreciably decreases as the nucleus mass number increases. The capture well is absent altogether in the case of the ^{208}Pb—^{208}Pb system. The shallowing and narrowing of a capture well in heavy systems, or even its absence, are explained by a substantial growth of the Coulomb energy of repulsion between nuclei, when the number of nucleons in them increases, which cannot be compensated by the corresponding growth of the nuclear attraction energy. As the mass number increases, the potential well shifts towards longer distances. In so doing, the minimum of the capture well becomes located at a distance, which, for light systems, is shorter than the sum of mean-square radii of interacting nuclei and, for medium and heavy systems, exceeds it (see Fig. 2).

In the "frozen density" approximation, the potential energy of interaction between nuclei sharply increases at distances shorter than the sum of the radii of the surfaces of the nuclei, which is caused by the substantial repulsion of the latter. This repulsion is a result of the nuclear matter compression and the strong density overlapping of interacting nuclei. The sharp growth of the potential energy stimulated by the strong density overlapping leads also to the density relaxation. Therefore, making use of the "frozen density" approximation, one may analyze nucleus–nucleus potentials $V(R)$ only in the vicinity of the barrier and at the touching point of nuclei. If the distance between nuclei is shorter, the "frozen density" approximation can be valid only at high collision energies.

The capture well plays an important role when two heavy nuclei collide. The nuclei cross the barrier rather quickly and become captured in the well at the initial stage of collision. In the capture well, various states of

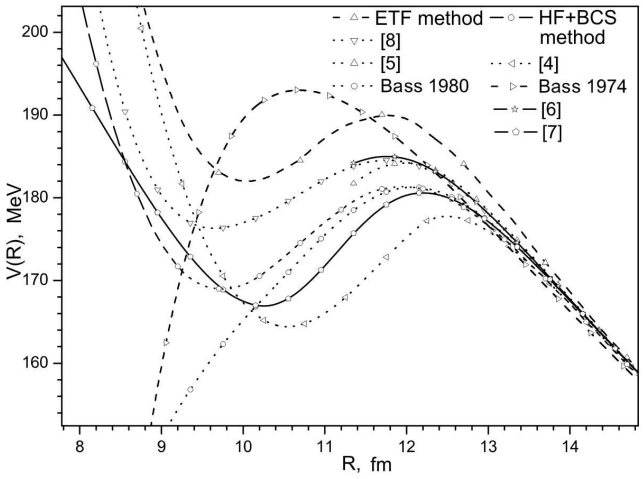

Fig. 4. Interaction potentials between ^{40}Ca and ^{208}Pb nuclei calculated in the ETF and HF+BCS approximations. The results of calculations of the interaction potential between the same nuclei making use of the expressions from works [1,4–8] are also depicted

the system of two strongly overlapped nuclei become occupied, and various processes, which are conditioned by different open reaction channels and determined by the probabilities of transitions between them, commence. The complicated excited system of strongly overlapped nuclei, which has been formed in the capture well, is the input channel for the formation of a nucleus or a fusion-fission reaction. The states formed in the capture well and connected with nuclei that fly apart give contributions to the elastic and various inelastic reaction channels. Whence, it follows that the absence of the capture well in the case of heavy systems leads to the change of the mechanism of the nuclear reaction course and makes the formation of the compound nucleus more difficult.

In Fig. 3, the interaction potentials $V(R)$ between a ^{40}Ca nucleus and five tin isotopes ^{100}Sn, ^{114}Sn, ^{118}Sn, ^{124}Sn, and ^{132}Sn, calculated in the ETF approximation, are shown. The neutron and proton densities for those Sn isotopes are depicted in this figure as well. As the mass number of Sn isotopes increases, the neutron distribution densities become more expanded; the same is true for the proton distribution densities, but to a lesser degree. This results in the formation of neutron clouds around the Sn isotopes with a large excess of neutrons. The indicated properties of the proton and neutron densities bring about the appearance of the strong isotopic dependence of the nuclear interaction potential. In particular, as the mass number of Sn isotopes increases, the barrier height decreases, and the potential capture well becomes deeper and "wider".

As was noted above (see also Fig. 1), the distributions of nucleon density calculated in the HF+BCS approximation possess a thicker diffusion layer of the nucleus, in comparison with those found in the ETF approximation. Therefore, it is useful to confront the potentials obtained in the framework of different approximations.

In Fig. 4, the interaction potentials between ^{40}Ca and ^{208}Pb nuclei, calculated in the HF+BCS and ETF approximations, are shown. The potential calculated in the HF+BCS approximation, if compared with that found in the semiclassical approximation, is characterized by a smaller height of the barrier and a deeper and wider capture well (see Fig. 4). The reason is that the nucleon density distributions calculated in the HF+BCS approximation possess a thicker diffusive layer of the nucleus, in comparison with that found in the semiclassical approximation. As a result of such a distribution of the nucleon densities, the nuclear interaction of nuclei at large distances between their surfaces turns out stronger in the HF+BCS approximation than that in the ETF one, while the Coulomb interaction is practically identical in both cases. The increase of the nuclear part of interaction between nuclei at large separations between their surfaces leads to a reduction of the barrier between them. Owing to a higher diffuseness of the nucleon density, the region, where the densities belonging to different nuclei strongly overlap, diminishes. As a result, the nuclear repulsion at short distances between interacting nuclei reduces, which leads to the widening and deepening of a well. This emphasizes the crucial influence of the diffuseness in the distribution of the nuclear matter density on the parameters of the interaction potential between nuclei.

For comparison, the interaction potentials calculated making use of simple expressions proposed in works [1, 4–8] are also presented in Fig. 4. The potentials that were suggested in works [5, 6] are determined only until the touching point of nuclei; therefore, they are plotted only up to this point, $R_t \approx 11.5$ fm. Figure 4 also exhibits the results that use the parametrizations of the potential proposed by Bass in 1974 and 1980 [1] and marked as *Bass 1974* and *Bass 1980*, respectively. One can see that the interaction potentials calculated in different approximations considerably differ from one another in the barrier region. Different parametrizations give different barrier heights, which results in the ambiguity of the description of the fusion and fusion-fission reactions of superheavy nuclei. We note that the halfwidth of the maximum in the cross-section

of the superheavy-nucleus formation reaction is about 3 MeV [30], which is much less than the uncertainty of the barrier height connected with the use of various theoretical approximations for the nucleus–nucleus interaction.

4. Diffuseness of the density distribution and the diffuseness of the nuclear part of the interaction potential between nuclei

4.1. Diffuseness of the density distribution and the properties of the nuclear interaction potential

In order to study the influence of the density diffuseness of colliding nuclei, which are in the ground state, on the nucleus—nucleus potential, let us parametrize the nucleon densities of nuclei in the ground states by the expression

$$\rho_{n(p)}(r) = \rho_{0n(p)}/\{1 + \exp[(r - R_{n(p)})/d]\}. \qquad (5)$$

Such a parametrization of the radial distribution of nucleon density has often been used in nuclear physics [31]. The parameters of this distribution $\rho_{0n(p)}$ and $R_{n(p)}$ were found by the direct variational method at a fixed value of the diffuseness d. By varying $\rho_{0n(p)}$ and $R_{n(p)}$, we minimized the nucleus binding energy calculated taking into account the gradient corrections to the kinetic energy functional for Skyrme forces SkP. The diffuseness d for the neutron and proton densities was varied within the interval from 0.5 to 0.8 fm with a step of 0.05 fm. The radial distributions of the neutron and proton densities of ^{64}Ni and ^{100}Mo nuclei in their ground states with such values of the diffuseness d are plotted in Fig. 5. These densities were used to calculate the interaction potentials between ^{64}Ni and ^{100}Mo nuclei, which are also displayed in this figure. While calculating the potentials, the ETF method with Skyrme forces SkP was used. For a comparison, the results of calculations of the potential between those nuclei, carried out in the HF+BCS approximation with Skyrme forces SkP, are shown (see Fig. 5).

At large distances between nuclei, the potential calculated in the HF+BCS approximation is close to the potential which uses the density parametrization (5) with the diffuseness $d = 0.55$ fm. However, at shorter distances, it is close to the potential calculated with the diffuseness of about 0.6 fm (see Fig. 5).

As the diffuseness of the density distribution grows, the potential capture well shifts towards longer distances between colliding nuclei, its depth increases, and the height of the potential barrier decreases. The reason is that the nucleon densities become more expanded as the density distribution diffuseness grows, so that the nuclear interaction at large distances between nuclei increases, and the barrier height decreases. As the density distribution diffuseness grows, the nuclear densities come into the strong overlapping at shorter distances between nuclei, so that the nuclear repulsion between nuclei, caused by the compression of the nuclear matter, decreases. This results in the widening and deepening of the capture well.

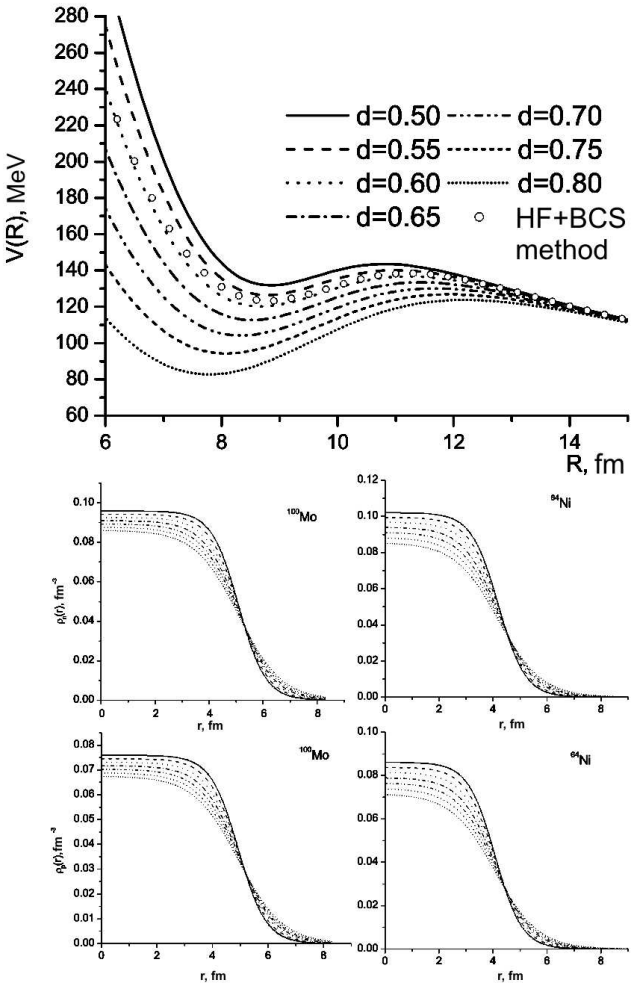

Fig. 5. Interaction potentials $V(R)$ for ^{64}Ni and ^{100}Mo nuclei for various values of the diffuseness d of the ground state densities calculated in the semiclassical approximation. For comparison, the interaction potential between nuclei found in the HF+BCS approximation with Skyrme forces SkP is shown, as well as the proton and neutron densities in the ground state for various d

The table shows the dependences of the potential barrier height and the bottom energy of the capture well on the diffuseness d of the ground state density. The potential barrier height decreases almost linearly with the growth of the diffuseness d, whereas the bottom energy of the capture well decreases much more quickly. The depth of the well, i.e. the difference between the barrier height and the well bottom, increases with the growth of d.

The HF+BCS approximation describes well the experimental radial distributions of the nucleon density; therefore, the potentials calculated making use of the density parametrization (5) with the diffuseness $d \approx 0.55 \div 0.6$ fm are close to the realistic one at various distances between nuclei.

4.2. Diffuseness of the potential and the nuclear fusion cross-section

The characteristics of nuclear reactions are often calculated making use of the Woods—Saxon parametrization of the nuclear part of the interaction potential between nuclei [1–3, 7, 18–20, 22–24]

$$V(R) = -V_0/\{1 + \exp[(R - R_{\rm pot})/a]\}. \quad (6)$$

Therefore, it is necessary to determine at what value of the parameter a the Woods—Saxon potential is close to the realistic potential found in the HF+BCS approximation. For this purpose, we determined first the parameters V_0, $R_{\rm pot}$, and a in Eq. (6) by fitting the potential which had been calculated in the ETF approximation with the value $d = 0.55$ fm for the diffuseness of the nucleon density distribution, in the range of distances R larger than the sum of nucleus radii R_t. Afterwards, we fixed the obtained value of $R_{\rm pot}$ and used it when fitting the potential which had been found in the ETF approximation for other values of the nucleon density distribution diffuseness. The dependences of V_0 and a on d given in the table were determined just in such a way.

Dependences of the potential barrier height $V_{\max}$, the bottom energy of the capture well $V_{\min}$, and the diffuseness a and the depths V_0 of the Woods—Saxon potential on the diffuseness d of the nucleon density in the ground state for the system ^{64}Ni+^{100}Mo

d, fm	$V_{\min}$, MeV	$V_{\max}$, MeV	V_0, MeV	a, fm
0.50	131.9	145.5	–73.18	0.74
0.55	126.5	139.1	–82.72	0.82
0.60	120.1	136.7	–93.33	0.89
0.65	112.7	132.4	–104.60	0.96
0.70	104.2	129.9	–116.90	1.03
0.75	94.3	126.8	–129.54	1.10
0.80	82.8	125.7	–143.22	1.17

The diffuseness a and the depth V_0 of the Woods—Saxon potential grow practically linearly as the nucleon density diffuseness d increases (see the table). The diffuseness of the nuclear part of the potential between nuclei, calculated by the ETF method and using Skyrme forces, is approximately 1.5 times larger at large distances than the diffuseness of the nucleon distribution in interacting nuclei.

As was pointed out above, the potential, which had been calculated using the nucleon density in form (5) for the density distribution $d = 0.55$ fm, corresponds at large distances to the potential determined for the HF distributions of nucleon density. This value of the density diffuseness corresponds to the diffuseness of the Woods—Saxon potential $a \approx 0.82$ fm (see the table). The Woods—Saxon potential agrees well at large distances with the nuclear part of the potential calculated in the ETF approximation for the density distribution diffuseness $d = 0.55$ fm. However, in the internal nucleus region, the Woods—Saxon potential tends to V_0. Therefore, they appreciably differ there.

The obtained value of the Woods—Saxon potential diffuseness, $a \approx 0.82$ fm, is in agreement with those proposed earlier. For example, the very close value of the diffuseness of the nucleus–nucleus potential at large distances, $a = 0.788$ fm, was found in work [8]. A somewhat smaller value of the diffuseness, $a = 0.7176$ fm, was obtained in work [5]. In work [7], by analyzing the elastic scattering of nuclei, the value $a = 0.657$ fm, which is very close to $a = 0.65$ fm proposed by Bass in 1980 [1], was found. In work [32], where the reactions of nuclear fusion were studied regularly, three values of the diffuseness have been proposed for light ($a = 0.481$ fm), medium ($a = 0.675$ fm), and heavy ($a = 0.895$ fm) systems of interacting nuclei. The analysis of data concerning the subbarrier fusion of various nuclei, carried out in works [22–26], led to rather large values of the diffuseness $a \approx 0.8 \div 1.5$ fm; and, while studying the subbarrier fusion of ^{16}O and ^{208}Pb nuclei, the value $a = 1.005$ fm was obtained [26]. The values of the diffuseness calculated in the case of the interaction between medium and heavy nuclei, which differ substantially from $a \approx 0.82$ fm, do not consist with the realistic distributions of the nucleon density in nuclei and nucleon–nucleon forces.

In order to investigate the influence of the potential diffuseness on the cross-section of near-barrier fusion, we fulfilled calculations for the reaction between ^{64}Ni and ^{100}Mo nuclei making use of the CCFULL code [20].

This computer program calculates the cross-sections of nuclear fusion taking into account the coupling between channels with low-located multipole surface-vibration excitations in both nuclei. In so doing, the nuclear part of the interaction potential between nuclei is parametrized in the form of the Woods–Saxon potential (6). The code takes into account the nonlinear effects of coupling with many-phonon multipole excitations of the surface. The parameters of the 2^+ and 3^- excitations, which are necessary for calculating the cross-sections with the help of the CCFULL code, were taken from the corresponding compilations of experimental data [33,34]. The parameters for the nuclear interaction potential were the same as in the table. The results of calculations and the experimental data are compared in Fig. 6. It is evident that the potentials calculated with small values of the density diffuseness result in the strongly underestimated cross-sections of fusion within the whole energy range. As the diffuseness of the nucleon density distribution d grows, the cross-section of fusion increases, which is connected with the lowering of the fusion barrier height. However, the slopes of the cross-section vs energy curves remain practically constant at subbarrier energies for various d. We emphasize that we did not intend to describe the fusion cross-section; our main purpose was to reveal the connection between the diffuseness of the density distribution, the diffuseness of the Woods–Saxon potential, and the fusion cross-section.

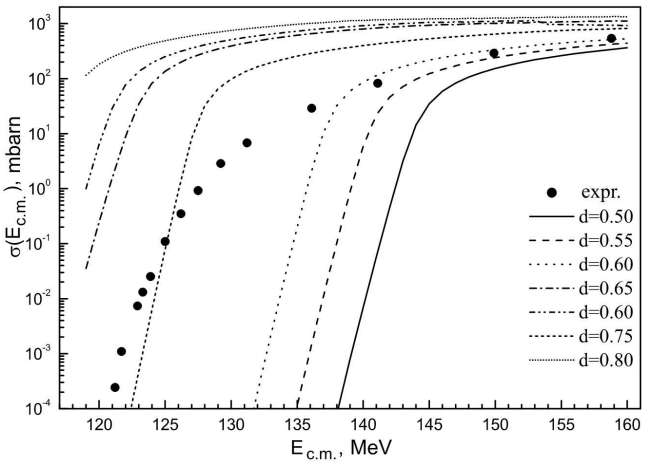

Fig. 6. Energy dependences of the cross-section of the nuclear fusion reaction ^{64}Ni+^{100}Mo for various diffusenesses d of the densities in the ground states of the nuclei

5. Conclusions

We have calculated the interaction potentials between nuclei in the framework of the HF+BCS theory and the ETF approximation, by making various assumptions concerning the nucleon density distribution in the ground state of nuclei. The obtained potentials were calculated in the "frozen density" approximation which is valid for the near-barrier and higher energies of collisions. The barrier heights agree well with various approximations that were proposed earlier for the nucleus–nucleus interaction. The variation of the isotopic composition of interacting nuclei has been demonstrated to affect the height and the thickness of the fusion barrier substantially.

The diffuseness of the nucleon density distribution in nuclei is rigidly bound with the diffuseness of the nuclear interaction potential. The diffuseness of the potential is approximately 1.5 times higher than that of the density distribution and is close to $a \approx 0.82$ fm. The values of the diffusenesses of the charge distribution and, owing to the isotopic symmetry, the neutron density distribution in medium and heavy spherical nuclei are practically constant and close to $d = 0.55$ fm (see Table 6.3 in work [31]). Therefore, the diffuseness of the potential in the case of the interaction between either medium or heavy spherical nuclei can accept neither very low nor very high values.

It has been shown that the parametrization of the nuclear part of the interaction potential between nuclei in the Woods–Saxon form is not satisfactory.

1. *Bass R.* Nuclear Reactions with Heavy Ions. — Berlin: Springer, 1980.
2. *Satchler G.R.* Direct Nuclear Reactions. — Oxford: Clarendon Press, 1983.
3. *Frobrich P., Lipperheide R.* Theory of Nuclear Reactions. — Oxford: Clarendon Press, 1996).
4. *Błocki J., Randrup J., Świątecki W.J., Tsang C.F.* // Ann. Phys. (N.Y.). — 1977. — **105**. — P. 427.
5. *Myers W.D., Swiatecki W.J.* // Phys. Rev. C. — 2000. — **62**. — P. 044610.
6. *Krappe H.J., Nix J.R., Sierk A.J.* // Ibid. — 1979. — **20**. — P. 992.
7. *Winther A.* // Nucl. Phys. A. — 1995. — **594**. — P. 203.
8. *Denisov V.Yu.* // Phys. Lett. B. — 2002. — **526**. — P. 315.
9. *Denisov V.Yu., Norenberg W.* // Eur. Phys. J. A. — 2002. — **15**. — P. 375.
10. *Ring P., Schuck P.* The Nuclear Many-Body Problem. — New York: Springer, 1980.
11. *Brack M., Guet C., Hakanson H.-B.* // Phys. Repts. — 1985. — **123**. — P. 275.
12. *Brack M., Bhaduri R.K.* Semiclassical Physics. — Reading, Massachusetts: Addison-Wesley, 1997.

13. *Denisov V.Yu., Nesterov V.O.* // Ukr. Fiz. Zh. — 2000. — **45**. — P. 1164; Yadern. Fiz. — 2002. — **65**. — P. 847.

14. *Nesterov V.A.* // Ukr. Fiz. Zh. — 2004. — **49**. — P. 225.

15. *Vautherin D., Brink D.M.* // Phys. Rev. C. — 1972. — **5**. — P. 626.

16. *Dobaczewski J., Flocard H., Treiner J.* // Nucl. Phys. A. — 1984. — **422**. — P. 103.

17. *Negele J.W.* // Rev. Mod. Phys. — 1982. — **54**. — P. 913.

18. *Dasgupta M., Hinde D.J., Rowley N. et al.* // Annu. Rev. Nucl. Part. Sci. — 1998. — **48**. — P. 401.

19. *Balantekin A.B., Takigawa N.* // Rev. Mod. Phys. — 1998. — **70**. — P. 77.

20. *Hagino K., Rowley N., Kruppa A.T.* // Comp. Phys. Communs. — 1999. — **123**. — P. 143.

21. *Denisov V.Yu.* // Phys. At. Nucl. 1999. — 62. — P. 1349; Eur. Phys. J. A. — 2000. — **7**. — P. 87.

22. *Hagino K., Rowley N., Dasgupta M.* // Phys. Rev. C. — 2003. — **67**. — P. 054603.

23. *Hinde D.J., Berriman A.C., Butt R.D. et al.* // Europ. Phys. J. A. — 2002. — **13**. — P. 149.

24. *Hinde D.J., Dasgupta M.* // Nucl. Phys. A. — 2004. — **734**. — P. 148.

25. *Newton J.O., R. D. Butt, M. Dasgupta et al.* // Phys. Rev. C. — 2004. — **70**. — P. 024605.

26. *Morton C.R., Berriman A.C., Dasgupta M. et al.* // Ibid. — 1999. — **60**. — P. 044608.

27. *de Vries H., de Jager C.W., de Vries C.* // At. Data Nucl. Data Tabl. — 1987. — **36**. — P. 495.

28. *Bertsch G.F.* // Z. Phys. A. — 1978. — **289**. — P. 103.

29. *Liang J.F., Shapira D., Gross C.J. et al.* // Phys. Rev. Lett. — 2003. — **91**. — P. 152701.

30. *Hofmann S., Munzenberg G.* // Rev. Mod. Phys. — 2000. — **72**. — P. 733.

31. *Barrett R.C., Jackson D.F.* Nuclear Sizes and Structure. — Oxford: Clarendon Press, 1977.

32. *Siwek-Wilczynska K., Wilczynski J.* // Phys. Rev. C. — 2004. — **69**. — P. 024611.

33. *Raman S., Nestor C.W., Tikkanen P.* // At. Data Nucl. Data Tabl. — 2001. — **78**. — P. 1.

34. *Kibedi T., Spear R.H.* // Ibid. — 2002. — **80**. — P. 35.

Received 04.10.05
Translated from Ukrainian by O.I. Voitenko

РОЗПОДІЛ ГУСТИНИ
ТА ПОТЕНЦІАЛ ВЗАЄМОДІЇ ЯДЕР

В.Ю. Денисов, В.А. Нестеров

Р е з ю м е

Детально досліджено потенціали взаємодії ядер, обчислені з використанням сил Скірма в рамках модифікованого наближення Томаса—Фермі і теорії Хартрі—Фока—БКШ. Показано, що величина ядерної частини потенціалу взаємодії між ядрами росте зі збільшенням кількості нейтронів в ізотопах, що зіштовхуються, і величини параметра дифузності розподілу густини взаємодіючих ядер. З ростом параметра дифузності розподілу густини взаємодіючих ядер відбувається зменшення висоти бар'єра між ядрами, збільшення глибини ями захоплення і поперечного перерізу злиття. Показано, що величина параметра дифузності ядерної частини потенціалу на великих відстанях між ядрами, обчислена із силами Скірма, перевищує величину параметра дифузності розподілу густини нуклонів у ядрах, що взаємодіють, приблизно у 1,5 раза. Реалістичні значення параметра дифузності ядерної взаємодії між середніми та важкими ядрами лежать в інтервалі $a \approx 0,75 \div 0,90$ фм.